arXiv:1603.08122v1 [cond-mat.mtrl-sci] 26 Mar 2016

An efficient ab-initio quasiharmonic approach for the thermodynamics of solids

Liang-Feng Huang, Xue-Zeng Lu, Emrys Tennessen, and James M. Rondinelli*
Department of Materials Science and Engineering,
Northwestern University, Evanston, IL 60208, USA

A first-principles approach called the *self-consistent quasiharmonic approximation* (SC-QHA) method is formulated to calculate the thermal expansion, thermomechanics, and thermodynamic functions of solids at finite temperatures with both high efficiency and accuracy. The SC-QHA method requires fewer phonon calculations than the conventional QHA method, and also facilitates the convenient analysis of the microscopic origins of macroscopic thermal phenomena. The superior performance of the SC-QHA method is systematically examined by comparing it with the conventional QHA method and experimental measurements on silicon, diamond, and alumina. It is then used to study the effects of pressure on the anharmonic lattice properties of diamond and alumina. The thermal expansion and thermomechanics of $Ca_3Ti_2O_7$, which is a recently discovered important ferroelectric ceramic with a complex crystal structure that is computationally challenging for the conventional QHA method, are also calculated using the formulated SC-QHA method. The SC-QHA method can significantly reduce the computational expense for various quasiharmonic thermal properties especially when there are a large number of structures to consider or when the solid is structurally complex. It is anticipated that the algorithm will be useful for a variety of fields, including oxidation, corrosion, high-pressure physics, ferroelectrics, and high-throughput structure screening when temperature effects are required to accurately describe realistic properties.

I. INTRODUCTION

Accurately simulating various anharmonic properties, i.e., thermal expansion and thermomechanics, of solids is important for obtaining a deep understanding of their plentiful thermal behaviors and for their realistic applications. The anharmonic properties can be derived from the volume and temperature dependences of the phonon spectra calculated using density-functional theory (DFT).[1] The most popular approach is the quasiharmonic approximation method (QHA),[2–4] where only the volume dependence is considered for the phonon anharmonicity, and temperature is assumed to indirectly affect phonon vibrational frequencies through thermal expansion. Here, the phonon spectra of about ten or more volumes are usually required for a typical QHA simulation, and the thermal expansion and thermomechanics are derived by fitting the free energy-volume relationship. In some cases, e.g., at high temperatures, high-order anharmonicity caused by multi-phonon coupling cannot be omitted as in the QHA method, and some more complicated and time-consuming methods, e.g., molecular dynamics,[5–12] self-consistent ab-initio lattice dynamics,[13,14] perturbative/nonperturbative renormalized harmonic approximations,[15–18] and vibrational self-consistent field calculations,[19] can be used to obtain the temperature-dependent phonons. Nonetheless, approximately ten or more volumes of such phonon spectra are also required to accurately calculate the thermal expansion and thermomechanics with the high-order anharmonicities.

Phonon calculations based on DFT forces are always time consuming, and prior to the actual calculation, various computational parameters[1,20] also need to be carefully tested to ensure convergence of the vibrational frequencies and anharmonicity, including the pseudopotentials, cutoff energy, k-mesh density, energy and force convergence thresholds, and supercell size in the small-displacement method[21,22] or the q-mesh density in the density-functional perturbation theory approach.[23,24] The general rule-of-thumb requiring ten or more volumes will make the anharmonic simulation, even when utilizing the simplest QHA method, rather computationally expensive, especially in some condensed matter fields where a large number of structures must be considered or the compound under study has a large unit cell, low symmetry, and numerous inequivalent atoms:

(i) In the fields of solid oxidation and corrosion, there are always many compounds (elements, oxides, hydroxides, oxyhydroxides, etc.) to consider[25–30] and each composition may have many polymorphs;[31–33]

(ii) In the high-pressure physics field, not only a wide range of volumes but also a large number of complex phases should be examined;[34–36]

(iii) For the metallic alloys field, the thermodynamics and mechanics of many phases at variable composition and temperature are always of concern;[37–39]

(iv) In the perovskite oxides,[40–42] ternary ceramics exhibit complex structures and large unit cells. The phonon calculations for an individual structure is already quite time consuming, not to mention the calculation of anharmonic properties in low-symmetry polymorphs; and

(v) In high-throughput screening and materials design[43–46] when including temperature effects, a huge number of compositions and structures should be calculated with a high efficiency-to-accuracy ratio.

To this end, these diverse fields require an efficient method

to accelerate the investigation of the anharmonic properties of related solids at finite temperatures.

In this work, we formulate an ab-initio method, called the *self-consistent quasiharmonic approximation* (SC-QHA) method, for achieving fast anharmonic calculations with high accuracy within the quasiharmonic approximation. Only the phonon spectra of two or three volumes are required in a SC-QHA calculation, which usually is much faster than the conventional QHA method. We carefully test the SC-QHA method using prototypical silicon, diamond, and alumina, and then also study the pressure effect on the anharmonic properties of diamond and alumina. Finally, we apply the SC-QHA method to accurately calculate the thermal expansion and thermomechanics of the structurally complex hybrid-improper ferroelectric $Ca_3Ti_2O_7$. Apart from the high efficiency, we show that the SC-QHA method is also very convenient for deciphering the microscopic physical origins of lattice dynamical and thermodynamic phenomena. Moreover, it can be readily transferred beyond the quasiharmonic realm to speed up the accurate first-principles simulation of thermal effects for the benefit of multiple fields in condensed-matter physics.

II. THERMODYNAMICS AND COMPUTATION

A. Theoretical Basis

The total Gibbs free energy ($G_{tot} = F_{tot} + PV$) of a crystal unit cell is expressed as

$$G_{tot}(P,T) = F_e(V,T) + F_{ph}(V,T) + PV\,, \qquad (1)$$

where P, $V = V(P,T)$, and T are the external pressure, unit-cell volume, and temperature, respectively; F_e and F_{ph} are the electronic and phononic Helmholtz free energies, respectively. To conveniently present the basic algorithm and efficiency of the SC-QHA method, only nonmagnetic insulators are considered here, where the electronic excitation and magnetic excitations are neglected. The transferability of the SC-QHA algorithm for solids with more complex degrees of freedom are discussed below. Therefore, $F_e(V,T)$ here equals the electronic energy $E_e(V)$ calculated from density functional theory (DFT) and $F_{ph}(V,T)$ is expressed as

$$F_{ph} = \frac{1}{N_q}\sum_{q,\sigma}\left\{\frac{\hbar\omega_{q,\sigma}}{2} + k_BT\log\left[1-\exp\left(-\frac{\hbar\omega_{q,\sigma}}{k_BT}\right)\right]\right\}, \qquad (2)$$

where k_B is the Boltzmann constant, N_q is the number of considered reciprocal points, $\omega_{q,\sigma}$ is the vibrational frequency of the σ-th phonon branch at the reciprocal coordinate q.

The equilibrium state under a specified external pressure P fulfills the relationship

$$\left.\frac{\delta G_{tot}}{\delta V}\right|_{P,T} = 0. \qquad (3)$$

Combining Eqs. 1, 2 and 3, we obtain an expression for the unit-cell volume

$$V(P,T) = \left[\frac{dE_e(V)}{dV} + P\right]^{-1} \times \frac{1}{N_q}\sum_{q,\sigma} U_{q,\sigma}\gamma_{q,\sigma}, \qquad (4)$$

where $U_{q,\sigma}$ and $\gamma_{q,\sigma} = -\frac{V}{\omega_{q,\sigma}}\frac{d\omega_{q,\sigma}}{dV}$ are the internal energy and Grüneisen parameter of the phonon mode (q,σ). (To guarantee that γ is calculated from the phonon modes with the same symmetry, $k{\cdot}p$ theory is used to identify and match the phonon branches obtained from different volumes according to the similarity of each mode's eigenvector.[47]) The physics underlying Eq. 4 is due to the balance between the external pressure P and internal pressure, i.e., electronic pressure ($P_e = -\frac{dE_e}{dV}$) plus the anharmonic phonon pressure ($P_\gamma = -\frac{dF_{ph}}{dV} = \frac{1}{VN_q}\sum_{q,\sigma} U_{q,\sigma}\gamma_{q,\sigma}$), such that

$$P = P_e(V) + P_\gamma(V,T). \qquad (5)$$

In the quasiharmonic approximation,[2–4] ω only depends on V such that the ω–V relationship can be described by a Taylor expansion (up to second order) as

$$\omega(V) = \omega(V_0) + \left(\frac{d\omega}{dV}\right)_0\Delta V + \frac{1}{2}\left(\frac{d^2\omega}{dV^2}\right)_0\Delta V^2, \qquad (6)$$

where V_0 is the reference volume and $\Delta V = V - V_0$. Then, we can derive the volume dependence of γ as

$$\gamma(V) = -\frac{V}{\omega}\left[\left(\frac{d\omega}{dV}\right)_0 + \left(\frac{d^2\omega}{dV^2}\right)_0\Delta V\right]. \qquad (7)$$

The calculation of the n-th order derivative of ω (i.e., $d^n\omega/dV^n$) requires the phonon spectra of $n+1$ volumes. With Eqs. 4, 6, and 7, the temperature-dependent unit-cell volume can be obtained in a self-consistent manner and it is this formalism which we call herein the self-consistent quasiharmonic approximation (SC-QHA) method. The complete derivation steps for the SC-QHA method, as well as the formula in the next section, can be found in the online Supplemental Material.

The SC-QHA method can also be viewed as an improved nonlinear Grüneisen model that is implemented in a self-consistent way. In a conventional Grüneisen model,[48–51] the linear ω–V relationship usually is considered, and during the calculation of the thermal-expansion coefficient $\alpha = \frac{1}{V}\frac{dV}{dT}$, the parameters V, ω, and γ are treated as constant. In addition, the zero-point vibration contribution to V is also absent in the Grüneisen model for $\alpha(T)$. Although a similar nonlinear ω–V relationship to that given shown in Eq. 6 has been used by Debernardi et al. for $\alpha(T)$ before,[52] the contribution of zero-point vibrations to V were omitted. Herein, both the zero-point vibrational contribution and nonlinear ω–V relationship are treated in the SC-QHA method (by Eqs. 4 and 6).

In principle, when we have an analytical expression for $\omega(V)$ (Eq. 6), $V(P,T)$ could be directly derived by minimizing the analytical G_{tot} (Eq. 1) with respect to V prior

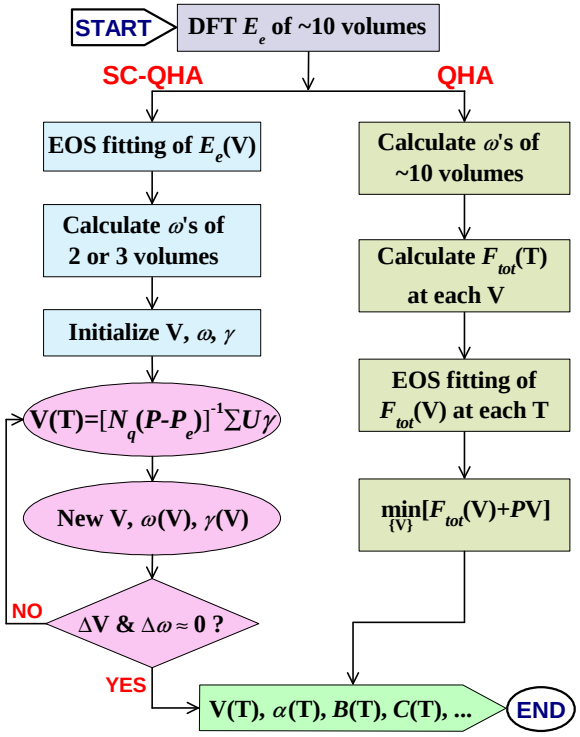

FIG. 1. The workflow chart for the SC-QHA method (left) compared to the conventional QHA method (right). Details of their algorithms are given in the main text.

to using Eq. 4. This approach should have a comparable numerical efficiency as the self-consistent method. However, the SC-QHA method is very convenient analytics method for which considerable physical information (as present in Eq. 4) can be obtained through the accompanying the iteration process or from the converged results; the SC-QHAD allows us to understand related properties and to further design materials. Indeed, the lowest-order SC-QHA method with γ kept constant, has been successfully used to reveal various anharmonic mechanisms in two-dimensional materials,[47,53–56] while we will show in this work that the higher-order SC-QHA method is necessary for three-dimensional solids at high temperatures (e.g., $\gtrsim$ 1000 K).

B. Computational Algorithm

The computational protocol for the SC-QHA method is depicted in Fig. 1, and described below:

(1) First, only the electronic energies (E_e) for approximately ten or more volumes are calculated using DFT. This step is required for both the SC-QHA and the conventional QHA methods.

(2) Next, the calculated E_e's are fit by an equation of state (EOS). There are various forms available, i.e., Birch-Murnaghan equation, modified Birch-Murnaghan equation, Birch equation, logarithmic equation, Murnaghan equation, Vinet equation, and Morse equation.[57] The fourth-order Birch-Murnaghan EOS is used here to produce an analytical $E_e(V)$ and $\frac{dE_e}{dV}$ expression.

(3) Phonon spectra of two and three volumes are calculated to obtain $(\frac{d\omega}{dV})_0$ and $(\frac{d^2\omega}{dV^2})_0$, respectively. The 1st-SC-QHA method only requires $(\frac{d\omega}{dV})_0$, whereas the 2nd-SC-QHA requires both $(\frac{d\omega}{dV})_0$ and $(\frac{d^2\omega}{dV^2})_0$.

(4) Prior to the self-consistent cycle, reasonable initial values for the unit-cell volume, phonon frequencies, and Grüneisen parameters are specified. To have a nonzero $\frac{dE_e}{dV}$ in the denominator of Eq. 4, the initial V is set to be the 0.2%-expanded DFT equilibrium V, which is used to calculate the initial vibrational frequencies (ω, Eq. 6) and Grüneisen parameters (γ, Eq. 7).

(5) The initial ω and γ values are used to calculate a new V using Eq. 4, and the new V is taken to recalculate phonon frequencies and Grüneisen parameters using Eq. 6 and 7, respectively. Then, the new ω's and γ's are used to further update the volume V, and this kind of self-consistent iteration continues until V and the ω's are converged to within an acceptable threshold (e.g., 10^{-4}%).

(6) The $V(T)$ relationship is then obtained when the specified temperature window is scanned during the self-consistent calculation, where the calculated V, ω's, and γ's at one temperature are used as the initial values for the next temperature.

After obtaining converged V, ω's, and γ's, then other thermodynamic properties may be calculated, e.g., the thermal-expansion coefficient, bulk modulus, heat capacity, free energy, entropy, etc. From Eq. 4, the volume thermal-expansion coefficient ($\alpha = \frac{1}{V}\frac{dV}{dT}$) is derived to be

$$\alpha = \frac{1}{N_q V B_T} \sum_{q,\sigma} C_{q,\sigma}\gamma_{q,\sigma}\,, \tag{8}$$

where B_T is the isothermal bulk modulus, and $C_{q,\sigma}$ is the isovolume heat capacity of the (q,σ) phonon mode. B_T can be expressed as the summation of four components

$$B_T = B_e + B_\gamma + B_{\Delta\gamma} + P_\gamma\,, \tag{9}$$

where $B_e = V\frac{d^2E_e}{dV^2}$ is the electronic bulk modulus; $P_\gamma = P - P_e$, as described above, is the anharmonic-phonon pressure, a first-order component; B_γ and $B_{\Delta\gamma}$ are the second-order components, and $B_{\Delta\gamma}$ results from the change of γ. B_γ and $B_{\Delta\gamma}$ are expressed as

$$\begin{aligned} B_\gamma &= -\frac{1}{N_q}\sum_{q,\sigma}\frac{dU_{q,\sigma}}{dV}\gamma_{q,\sigma} \\ &= \frac{1}{N_q V}\sum_{q,\sigma}\left(U_{q,\sigma} - C_{q,\sigma}T\right)\gamma_{q,\sigma}^2 \end{aligned} \tag{10}$$

and

$$B_{\Delta\gamma} = -\frac{1}{N_q}\sum_{q,\sigma} U_{q,\sigma}\frac{d\gamma_{q,\sigma}}{dV} \tag{11}$$
$$= -\frac{1}{N_q V}\sum_{q,\sigma} U_{q,\sigma}\left[(1+\gamma_{q,\sigma})\gamma_{q,\sigma} - \frac{V^2}{\omega_{q,\sigma}}\frac{d^2\omega_{q,\sigma}}{dV^2}\right],$$

where $\frac{d^2\omega_{q,\sigma}}{dV^2}$ equals zero in the 1st-SC-QHA method. In addition, by obtaining the thermal expansion and isothermal thermomechanics, the isoentropic thermomechanics can also be readily derived.[51,58,59] Note that the mechanical properties obtained from experimental measurements always reside between the isothermal and isoentropic limits, and this work mainly focuses on the introduction of the SC-QHA method rather than focusing on the detailed mechanical relationships.

To realize a faster SC-QHA calculation, we self-consistently solve Eq. 4 for V at very low temperature (e.g., 0.1 K), and then use $\alpha(T)$ to obtain V at higher temperatures, i.e.,

$$V(T+\Delta T) = (1+\alpha\cdot\Delta T)V(T), \tag{12}$$

which help us avoid the self-consistent calculation for each temperature. A temperature increment (ΔT) of $\lesssim 2.0$ K can yield converged results.

The numerical implementation of the code is written in FORTRAN and can be accessed via a GitHub Repository at http://github.com/MTD-group under GPLv3.

1. *Comparison to the Conventional QHA Approach*

In the conventional QHA method (see Fig. 1, right column),[2–4] the phonon spectra for approximately ten or more volumes, especially for accurate thermomechanics, are required to be calculated, from which the F_{tot} of each volume within a specified temperature window is calculated. Then, an EOS is used to fit the calculated $F_{tot}(V)$ at each considered temperature. Finally, $G_{tot} = F_{tot}+PV$ is minimized with respect to V at each considered temperature, which yields various thermodynamic properties, e.g., $V(T)$, $\alpha(T)$, and $B(T)$. Such process is needed in both testing convergence parameters and in performing meaningful QHA calculations. However, the 1st-SC-QHA method using phonon spectra of only two volumes can be efficiently used in such test calculations. After the optimal numerical and computational parameters are determined, the 2nd-SC-QHA method using phonon spectra of three volumes may then be used to simulate accurate thermodynamic quantities.

2. *Extension to Metallic and Magnetic Crystals*

Herein nonmagnetic insulators are considered, however, in metals[60,61] and magnetic solids,[62–73] electronic and magnetic excitations, as well as spin-phonon coupling, at finite temperatures should be considered in computing the thermodynamic properties. For the SC-QHA simulation of a metal, we need to additionally treat the derivatives of $F_e(V,T)$ in a similar way as $F_{ph}(V,T)$; the electronic Grüneisen parameters[51] also need to be calculated. The main difference is that the Fermi-Dirac distribution should be used for the electrons in F_e, while the Bose-Einstein distribution is used for the phonons in F_{ph}.

For magnetic solids, the ensemble of magnetic configurations and the spin-phonon coupling should be correctly considered at finite temperatures, while the volume dependence of the phonon spectra is similarly calculated as that for nonmagnetic solids.

3. *Extension to High-Order Anharmonic Cases*

In the quasiharmonic approximation, where $\omega = \omega(V)$, only the low-order anharmonicity of phonons is considered.[74] When multi-phonon interactions are considerable, especially at very high temperatures, the phonon frequency has an additional explicit temperature dependence, i.e., $\omega = \omega(V,T)$, and some expensive methods beyond the quasiharmonic approximation, as described in the Introduction, should be used to capture such high-order anharmonicity. In the calculation of high-order anharmonic thermal expansion and thermomechanics, if the free-energy EOS fitting algorithm in the conventional QHA method is adopted, the anharmonic phonon spectra of ten or more volumes are required for an accurate fit. Alternatively, the Taylor-expansion and self consistency algorithms in the SC-QHA method can be used to efficiently describe the volume dependence of the anharmonic phonons, and the computational expense for high-order anharmonic cases will be significantly reduced.

C. Density-Functional Calculations

The Vienna *Ab Initio* Software Package (VASP)[20,75,76] is used to calculate the energies, forces, and stresses at the DFT level. The projector augmented-wave (PAW) method[77,78] is used to treat the interaction among the core and valence electrons and a planewave cutoff energy of 800 eV is also used. The electronic exchange-correlation potential is described by the PBEsol[79,80] parameterization, which we find generally gives more accurate thermodynamic quantities.[81] We use a reciprocal-grid density of $\approx \frac{30}{a}\times\frac{30}{b}\times\frac{30}{c}$, where a, b, and c are the lattice constants of the periodic cell scaled by the unit of angstrom. The convergence thresholds for the electronic energy and force are 5×10^{-8} eV and 5×10^{-4} eV Å^{-1}, respectively. The atomic positions, cell volume, and cell shape are globally optimized for the equilibrium states, and only the atomic positions and cell shape are optimized for a solid at a compressed/expanded volume.

The PHONOPY code[3,4] is used to calculate phonon spectra, where the small-displacement method[21,22] is im-

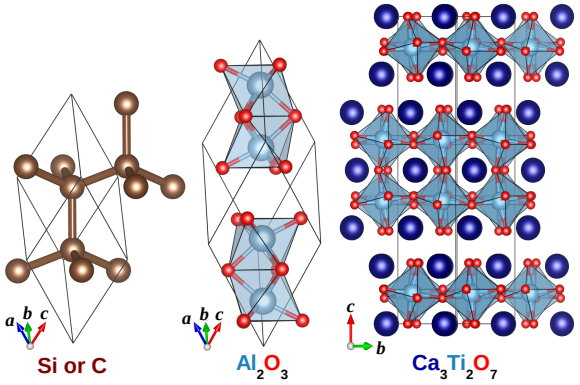

FIG. 2. The structures for silicon (diamond), alumina, and $Ca_3Ti_2O_7$, where the unit cells are indicated by the black empty parallelepipeds.

plemented, and the atomic displacement amount is set to be 0.03 Å. The supercells for the phonon calculation of Si, C, Al_2O_3, and $Ca_3Ti_2O_7$ are $5\times5\times5$ (250 atoms), $3\times3\times3$ (54 atoms), $2\times2\times2$ (80 atoms), and $2\times2\times1$ (192 atoms) times their respective unit cells (Fig. 2, see also Supplemental Material). For the conventional QHA calculation, 14, 11, and 18 volumes are considered for Si, C, and Al_2O_3 (see Supplemental Material).

The unexpected large supercell of Si is required for its accurate anharmonic properties according to our fast 1st-SC-QHA benchmark calculations; the underlying physical origin is due to the existence of variable negative Grüneisen parameters in its Brillouin zone (see Supplemental Material). The LO–TO splitting has negligible effect on the anharmonic properties according to our SC-QHA test calculations on Al_2O_3 (Supplemental Material), because only the LO because only the LO phonons in a very small reciprocal space close to the Γ point are affected.[82,83]

For the 2nd-SC-QHA calculation, the phonon spectra of the equilibrium, 3.0%-compressed, and 3.0%-expanded volumes are used for Si, C, and Al_2O_3, where the later two volumes are used for the 1st-SC-QHA calculation. When $Ca_3Ti_2O_7$ is under expansion, portions of the acoustic phonon branches will be spuriously softened and become dynamically unstable in the DFT calculation (Supplemental Material). However, in experimental measurement,[84] $Ca_3Ti_2O_7$ has no phase instability during its thermal expansion up to temperatures as high as its decomposition temperature (1150 K). Thus, it should be the increased phonon-phonon coupling upon heating that stabilizes those acoustic phonons and makes them behave normally, which is quite similar to what occurs in TiO_2.[85–87] To avoid this kind of phonon anomaly in expanded $Ca_3Ti_2O_7$, the phonon spectra of the equilibrium, 1.5%-compressed, and 3.0%-compressed volumes are used in the SC-QHA calculation of $Ca_3Ti_2O_7$. In addition, the conventional QHA method cannot be used when there is any instability in the quasiharmonic DFT phonons. This is also a numerical advantage of the SC-QHA method compared to the conventional QHA method.

III. RESULTS AND DISCUSSION

A. Algorithm Benchmarks

The calculated volume thermal-expansion coefficient (α), isobaric heat capacity ($C_p = C_v + TV_T B_T \alpha^2$),[59] and isothermal bulk modulus (B_T) obtained from the 1st-SC-QHA, 2nd-SC-QHA, and QHA methods for silicon (Si), diamond (C), and alumina (Al_2O_3) under zero pressure and at temperatures from 0 K to the melting point, T_m, are shown in Fig. 3. The low-temperature variations in $\alpha(T)$ and detailed analysis of B_T are given in Fig. 4. The available experimental results for Si, C, and Al_2O_3[88–108] are also collected to compare with the calculated values in Fig. 3 and 4. The raw data is available in digital format in the Supplemental Material.

1. *Thermal Expansion Coefficients*

All three methods generally perform well for α when compared with experimental measurements [Fig. 3(a,d,g)]. If we use the QHA results as the theoretical reference for our proposed method, then we find that the 2nd-SC-QHA approach has a higher accuracy than the 1st-SC-QHA method.

At temperatures of $\leqslant 300$ K, the $\alpha(V)$ curves from these three methods are in excellent agreement with each other and the experimental results, allowing for a scattering of $\lesssim 2\times10^{-6}$ K^{-1} in experimental data [Fig. 4(a,b,c)]. At temperatures of $\leqslant \frac{1}{4}T_m$, the 2nd-SC-QHA (1st-SC-QHA) thermal expansion coefficients deviate from the QHA ones only by 0.4% (-3.6%), 2.7% (4.9%), and 2.6% (4.3%) for Si, C, and Al_2O_3, respectively [Fig. 3(a,d,g)]. Thus, both the 1st-SC-QHA and 2nd-SC-QHA methods have high accuracy for the thermal expansion at relatively low temperatures. At higher temperatures, e.g., $\frac{2}{3}T_m$, the thermal expansion coefficients obtained from the 2nd-SC-QHA (1st-SC-QHA) deviate from the QHA ones by 1.5% (-6.5%), 6.3% (13.0%), and 4.2% (10.1%) for Si, C, and Al_2O_3, respectively [Fig. 3(a,d,g)], which indicates that the 2nd-SC-QHA method should be preferred to the 1st-SC-QHA method when seeking to achieve an accurate simulation of the thermal expansion at relatively high temperatures.

Here we note that it is also quite challenging to measure α accurately in experiment, especially at high temperatures, and the scatter in the experimental data always significantly increases with temperature. In fact, the theory-experiment discrepancy is even smaller than the experimental uncertainty [Fig. 3(a,d,g)]. Apart from some possible theoretical factors (e.g., the exchange-correlation potential and the quasiharmonic approximation itself) causing the inaccuracies in the simulated thermal expansion coefficients, there are also many experimental

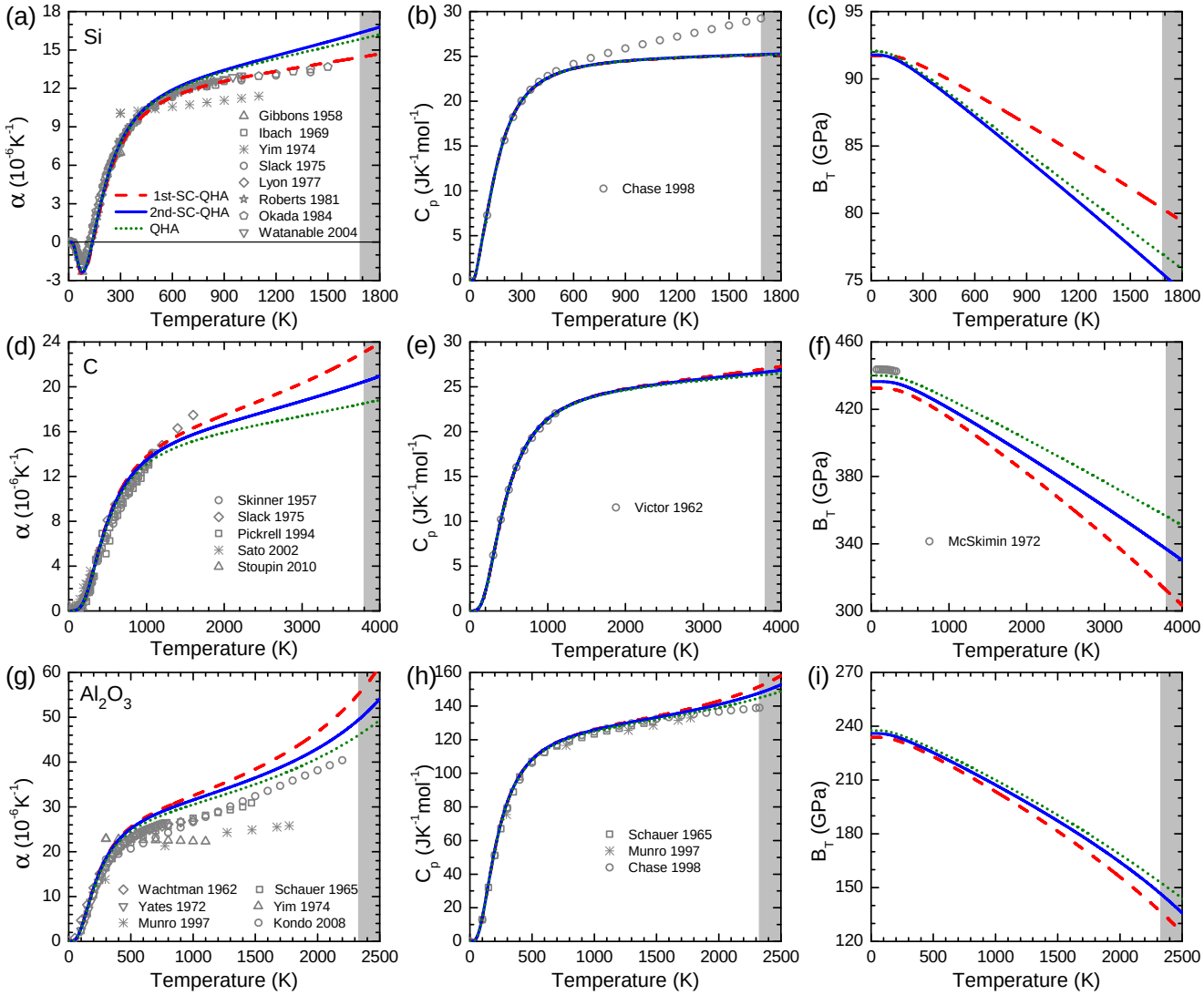

FIG. 3. The volume thermal-expansion coefficient (α), isobaric heat capacity (C_p), and isothermal bulk modulus (B_T) of (a–c) Si, (d–f) diamond, and (g–i) alumina, where the areas with temperatures above the melting points are shaded in gray. The experimental,[88–107] 1st-SC-QHA, 2nd-SC-QHA, and QHA results are presented by symbols, dashed red lines, solid blue lines, and dotted green lines, respectively. The experimental results are also tabulated for accessibility in the Supplemental Materials.

factors that can influence the measurement accuracy. First, thermal expansion always varies with the crystalline orientation.[93,102] When the crystalline orientation is not well characterized, the derived thermal expansion may vary among single crystals, powders, and polycrystals. Second, the measured samples are readily contaminated by various impurities (e.g., Cu, Fe, Mg, Ca, etc.), which may have profound effect on thermal expansion.[93,96,101,102,104,109,110] Next, the precipitation of some metastable phases in the sample at relative high temperatures may influence the thermal expansion. For example, there are many polymorphs (e.g., α, θ, γ, and δ phases) of Al_2O_3,[111,112] and the relative stability among the polymorphs correlates with temperature and impurity concentration.[112,113] It also has been found that the metastable θ-Al_2O_3 has a smaller thermal expansion than the stable α-Al_2O_3,[83] which may be related with the fact that the experimental thermal expansion is always smaller than the simulated one for α-Al_2O_3 [Fig. 3(g)].

Moreover there are many methods to measure the thermal expansion of solids, e.g., push-rod dilatometer,[99] capacitance dilatometer,[93,98,114] interferometric dilatometer,[89,93,99,105] and X-ray diffraction.[88,96,97,100,101,104,107,108] Although an accuracy from 10^{-6} to 10^{-8} K^{-1} may be declared for each measurement, the discrepancy between different measurements still can be on the order of 10^{-6} K^{-1}. Last, the thermal-expansion coefficient is derived from the lattice-constant variation with temperature, where analytical functions are used for the data fitting.[96,98] When the data is insufficiently large and exhibits obvious scatter, the derived α will also depend on the chosen

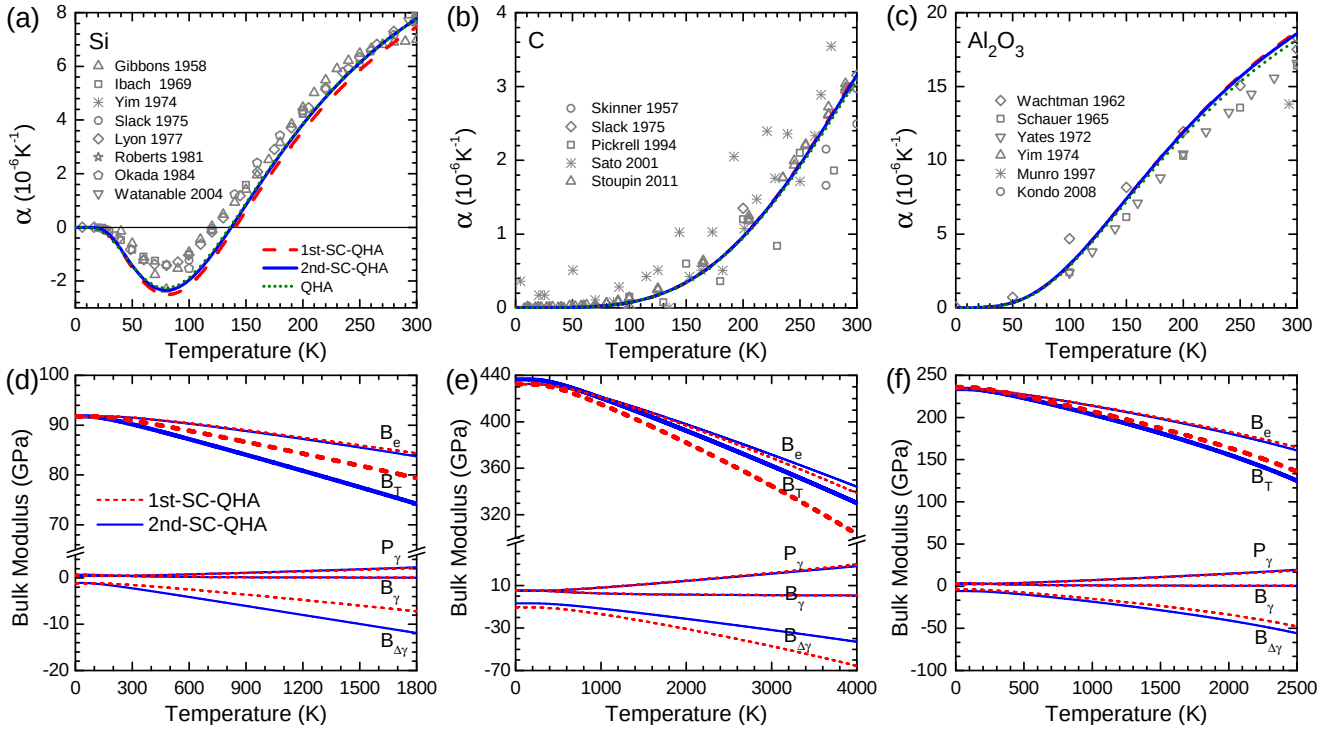

FIG. 4. The variations of α at low temperatures and B_T components (B_e, B_γ, $B_{\Delta\gamma}$, and P_γ) for (a,d) silicon, (b,e) diamond, and (c,f) alumina. In panels (a–c), the three calculated curves nearly overlap and are close to the experimental results.[88–107]

fitting function. For example, a difference of several percentages can be readily found when refitting the data reported by Yim.[96]

Most of the available experimental thermal expansion coefficients for these compounds are reported in earlier reports (e.g., 1950–1980s), and high-temperature data are still scarce, which makes stringent experiment–experiment and theory–experiment comparisons difficult. Therefore, accurate experimental measurements (especially for high temperatures) on high-quality samples are still needed to precisely understand the thermal expansion of many solids. Nonetheless, according to our current comparison, we find that relatively high accuracy is achieved by the 2nd-SC-QHA method (or even by the 1st-SC-QHA method), which only requires the phonon spectra of three (or two) volumes, rather than ten or more volumes as in the conventional QHA method.

2. *Isobaric Heat Capacity*

In addition to the good performance of the SC-QHA method for the thermal expansion coefficients, both the 1st-SC-QHA and 2nd-SC-QHA methods also yield highly accurate isobaric heat capacities for Si, C, and Al_2O_3, with respect to the QHA results [Fig. 3(b,e,h)]. The simulated C_p values are also consistently agree with the experimental ones for C and Al_2O_3 [Fig. 3(e,h)], although the experimental C_p for Si gradually deviates from the simulated one at temperatures $\gtrsim$ 500 K, e.g., by 8.3% at $\frac{2}{3}T_m$ (1124 K).

Usually the experiment–theory discrepancy for Si is ascribed to the omission of high-order anharmonicity beyond the quasiharmonic approximation, and an *ad-hoc* anharmonic correction of 8% for the heat capacity has been suggested.[115,116] However, such a simple anharmonic correction for heat capacity will adversely influence the accuracy of the theoretical α: When the quasiharmonic heat capacity is corrected by 8%, the quasiharmonic α also correspondingly needs to be increased by about 8% (Eq. 8).[117] Because the quasiharmonic α for Si is already higher than the experimental one. e.g., by 8% at $\frac{2}{3}T_m$, Fig. 3(a), such a correction will further increase the theory-experimental discrepancy in α by $\sim$16% at $\frac{2}{3}T_m$.

These results then motivate for a more systematic and improved understanding of the anharmonic properties of Si. Apart from obtaining perhaps more precise experimental measurements on high-quality samples, state-of-art ab-initio simulations of the high-order anharmonicity are needed; here, our SC-QHA algorithm may be used to speed up the calculation of the volume dependence of the anharmonic phonon spectra needed for those higher level theories.

3. *Isothermal Bulk Modulus*

An anticipated thermal softening of materials is observed in the temperature dependence of B_T [Fig. 3(c,f,i)]. From 0 K to $\frac{2}{3}T_m$, the softening of the isothermal bulk

moduli for Si, C, and Al_2O_3 are 6.8, 69.6, and 55.3 GPa from the 1st-SC-QHA method, 10.1, 59.9, and 51.3 GPa from the 2nd-SC-QHA method, and 9.7, 51.3, and 49.7 GPa from the QHA method, respectively. Although each method results in the same qualitative chemical trends for B_T, the 2nd-SC-QHA method gives a higher quantitative accuracy than the 1st-SC-QHA method with respect to the QHA method.

We understand this improved precision obtained by the 2nd-SC-QHA method as follows: The B_T is calculated from the second derivative of the free energy; thus, it is sensitive to both the method type and the number and range of cell volumes chosen in the QHA method. Nonetheless, the difference between the 2nd-SC-QHA and QHA results is already smaller than the numerical uncertainty in the QHA method (Supplemental Material).

In addition, the SC-QHA method enables us to decompose B_T into four contributing components (Eq. 9), i.e., B_e, P_γ, B_γ, and $B_{\Delta\gamma}$, where $B_{\Delta\gamma}$ results from the change of the Grüneisen parameter. The bulk moduli for Si, C, and Al_2O_3, as well as their corresponding components, are shown in Fig. 4(d,e,f), where the 1st-SC-QHA and the 2nd-SC-QHA results are compared. It can be clearly discerned that the difference between the bulk moduli obtained from the 1st-SC-QHA and the 2nd-SC-QHA mainly originates from deviations in the calculated $B_{\Delta\gamma}$, indicating the importance of the nonlinear vibrational frequency variation in solid thermomechanics. Moreover, B_e is consistently larger than B_T, indicating that the excitation of anharmonic phonons (i.e., $P_\gamma+B_\gamma+B_{\Delta\gamma}$) has a net softening effect on the bulk modulus. Therefore, beyond achieving a higher computational efficiency, the SC-QHA method also provides a convenient and complementary approach to the conventional QHA for uncovering the physical origins of thermomechanics.

B. Algorithm Applications

1. *Pressure Dependent Anharmonicity*

In high-pressure physics, the external pressure is controlled by compressing a diamond anvil cell (DAC), and the optical spectra of a ruby (Cr-doped Al_2O_3) particle adjacent to the sample is used to calculate the actual pressure in the DAC.[118–121] Thus, it is useful to study the pressure dependence of the anharmonic properties of C and Al_2O_3. When using the conventional QHA method to study the pressure effect, a large range of volumes should be considered, and the phonon spectra of numerous volumes probably need to be calculated to give confidence to the results. Considering extra volumes far away from the equilibrium volume, however, will introduce some numerical error to the QHA results for zero and low pressures, because of the decreased weights of the equilibrium and slightly-compressed volumes in the EOS fitting process (Supplemental Material). Thus, simulating the pressure-dependent anharmonic properties using the QHA method

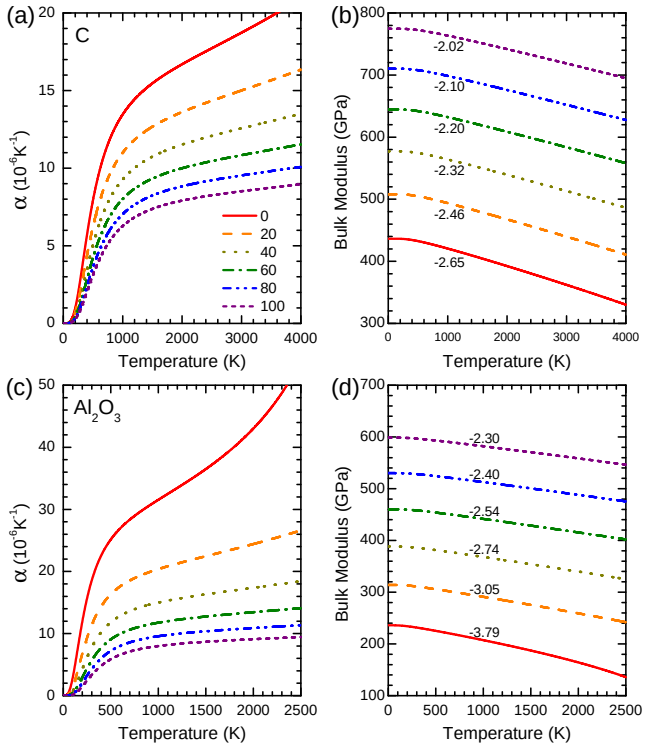

FIG. 5. Pressure dependence of α and B_T for (a,b) diamond and (c,d) alumina, where the slopes (in 10^{-2} GPa/K) of the B_T curves at 1000 K are indicated.

is not only computationally expensive, but also prone to intrinsic numerical uncertainties from the EOS fitting.

Here we remedy the shortcomings of the conventional QHA and apply our 2nd-SC-QHA method to examine the pressure effects on $\alpha(T)$ and $B_T(T)$ for C and Al_2O_3 from 0–100 GPa (Fig. 5). We find that α decreases with increasing pressure [Fig. 5(a,c)], which is mainly due to the increased B_T according to Eq. 8 and Fig. 5(b,d). The phonon mode hardening and the corresponding decrease in phononic anharmonicity also makes a minor contribution to the pressure-induced decrease of the thermal expansion coefficient. Interestingly, $\alpha(Al_2O_3)$ is approximately two times that of α(C) at 0 GPa, while they become comparable at 100 GPa, because of the faster stiffening rate of $B_T(Al_2O_3)$ with pressure. B_T increases with increasing pressure, but decreases with increasing temperature. The thermal-softening rate given by $-dB_T/dT$ decreases with increasing pressure [Fig. 5(b,d)], because of the decreased phonon anharmonicity. When the thermal effects on α and B_T are comparable with or even larger than the pressure effect, the simulated results for C and Al_2O_3 here will be useful for the high-pressure experiments carried out under variable temperature.

2. *Anharmonicity in Complex Ceramics*

The accuracy of the SC-QHA method for Si, C, and Al_2O_3, as well as its application to C and Al_2O_3 under pressure, motivate us to study the thermal expansion and thermomechanics of $Ca_3Ti_2O_7$. This compound is an important hybrid-improper ferroelectric (HIF)[122] that has received considerable attention recently.[123] Its thermal expansion has also been recently measured in experiment.[84]

The calculated $V(T)$, $\alpha(T)$, and $B_T(T)$ from both the 1st-SC-QHA and 2nd-SC-QHA methods are shown in Figure 6. We find that the 1st-SC-QHA results deviate from the 2nd-SC-QHA ones, indicating the importance of the nonlinear frequency-volume variation in this ferroelectric material. Thus, it is necessary to use the 2nd-SC-QHA method for such kind of HIFs where multiple lattice modes interact to stabilize the ferroelectric phase. Therefore, we focus our discussion on the results obtained from the 2nd-SC-QHA method below.

In Fig. 6(a), our theoretical $V(T)$ variation is compared with the measured temperature-dependent volume data collected from two experiments (labeled as "Senn Expt 1" and "Senn Expt 2") by Senn *et al.*,[84] one of which (Senn Expt 2) was provided by Senn and co-workers through private communications after publication of Ref. 84. These two sets of experimental data have no observable deviation, though according to Senn's comments, the X-ray wavelengths used for these two sets of measurements are slightly different, which may introduce a normalization error in the X-ray diffraction analysis. The 2nd-SC-QHA unit-cell volume is about 0.4% higher than Senn's measurements, indicating the high accuracy of our simulation.

To facilitate a direct theory-experiment comparison for $V(T)$, the experimental data sets are uniformly shifted upwards by 2.3 Å^3, such that the lowest temperature experimental data coincides with our 2nd-SC-QHA $V(T)$ curve as shown in Fig. 6(b). We find that our 2nd-SC-QHA $V(T)$ curve perfectly overlaps with the experimental temperature variation, except for a narrow temperature range, where a very small kink centered at 360 K appears [Fig. 6(b), inset].

To have a direct theory-experiment comparison for α, we extract the α from the experimental data in two ways. First, we calculate α from the differential between two neighboring data, i.e.,

$$\alpha\left(\frac{T_1+T_2}{2}\right) = \frac{2}{V_1+V_2}\frac{V_1-V_2}{T_1-T_2}\,. \qquad (13)$$

Second, we analytically derive $\alpha = \frac{1}{V}\frac{dV}{dT}$ from a fitted $V(T)$ curve using an exponential function of the form $\sum_{i=0}^{3} s_i T^i$. All the experimental thermal expansion data agree well with our 2nd-SC-QHA $\alpha(T)$ curve [Fig. 6(c)], except for some scattering in experimental data above 300 K caused by the presence of the kink in $V(T)$ [Fig. 6(b)]. This experimental kink may indicate some unknown processes, e.g., impurities and domain dynamics, becoming thermally activated in the sample above 300 K,

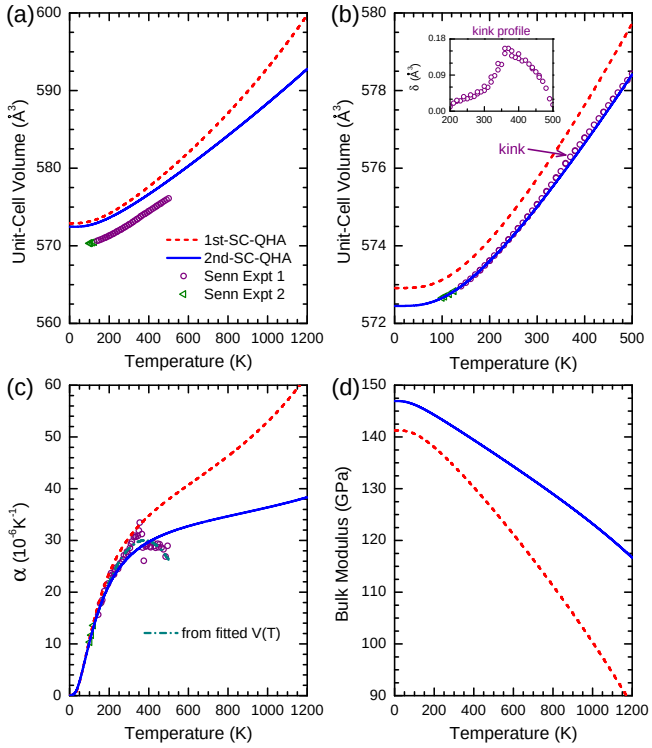

FIG. 6. Temperature dependence of the (a,b) unit-cell volume, (c) thermal expansion coefficient, and (d) bulk modulus of $Ca_3Ti_2O_7$, where the experimental results are shifted in panel (b) to facilitate comparisons. The first set of experimental results ("Senn Expt 1") are taken from Ref. 84 and the second data set ("Senn Expt 2") was provided by Senn through a private communication. The inset of panel (b) shows a detailed profile of the experimental kink at 360 K, where δ is the difference between the shifted experimental $V(T)$ data and the 2nd-SC-QHA calculate profile.

or certain small uncontrollable uncertainty in the experimental characterization. Upon decreasing temperature, α decreases down to zero at 0 K [Fig. 6(c)], thus, the $V(T)$ variation becomes less dispersive [Fig. 6(b)]. This is an inevitable quantum-mechanical effect, where fewer quantized phonons are thermally excited upon cooling.

Last, from both experimental measurements and our SC-QHA simulation, no negative thermal expansion is observed in $Ca_3Ti_2O_7$. This has been ascribed by Senn[84] to the octahedra tilting (X_3^- symmetry) being frozen out in the $Cmc2_1$ (or equivalently $A2_1am$ symmetry) phase in the Ruddlesden-Popper (RP) $A_3B_2O_7$ (A=Ca and B =Ti or Mn) compounds. For a more complete understanding of the thermal expansion and other anharmonic properties of $Ca_3Ti_2O_7$, further experimental measurements and more detailed analysis are still required.

IV. CONCLUSIONS

A fast and accurate ab-initio method called the self-consistent quasiharmonic approximation (SC-QHA)

method has been formulated to calculate various anharmonic properties of solids at finite temperatures. The SC-QHA method not only is about five times per dimension faster than the conventional QHA method, but also aids in the physical analysis of underlying anharmonic mechanisms. Although we showed the superior performance of the SC-QHA method compared to the conventional QHA using nonmagnetic insulators, the methodology can be readily extended to metallic and magnetic solids, where electronic and magnetic excitations are also important. Moreover, the basic SC-QHA algorithm can be transferred to the realm beyond the quasiharmonic approximation, i.e., to compute high-order anharmonicities, and reduce the computational overhead for the simulation of high-order anharmonic properties.

The efficiency and accuracy calibrations of the SC-QHA method based on silicon, diamond, and alumina show that the 2nd-order SC-QHA method is systematically more accurate than the 1st-order SC-QHA implementation, but the 1st-SC-QHA method is useful for testing the computational parameters required in a density functional theory calculation. After evaluating the SC-QHA method, we examined the pressure-dependent thermal expansion and thermomechanics of diamond and alumina, which are two important materials in high-pressure physics. Finally, the SC-QHA method was also used to study the thermal expansion and thermomechanics of $Ca_3Ti_2O_7$, which is structurally complex and computationally challenging for the conventional QHA method. No negative thermal expansion was found in $Ca_3Ti_2O_7$, which is consistent with a recent experimental measurement. The simulated $V(T)$ variation also precisely agrees with available experimental data. These results demonstrate that the SC-QHA method is both an efficient computational and useful theoretical tool to understand experimentally determined anharmonic properties of materials.

ACKNOWLEDGMENTS

L.-F.H. and J.M.R. wish to thank Dr. M. Senn (University of Oxford), and Prof. S.-W. Cheong (Rutgers University) for providing additional experimental data for $Ca_3Ti_2O_7$, as well as for the helpful e-mail exchanges. L.-F.H. and E.T. were supported by the Office of Naval Research MURI "Understanding Atomic Scale Structure in Four Dimensions to Design and Control Corrosion Resistant Alloys" under Grant No. N00014-14-1-0675. X.-Z.L. and J.M.R. were supported by the National Science Foundation (NSF) through the Pennsylvania State University MRSEC under award number DMR-1420620. Calculations were performed using the QUEST HPC Facility at Northwestern University and the HPCMP facilities at the Navy DoD Supercomputing Resource center.

CONTRIBUTIONS

The study was planned, methods formulated, calculations carried out, and the manuscript prepared by L.-F.H. and J.M.R. X.-Z.L. and E.T. performed analyses on $Ca_3Ti_2O_7$ and Al_2O_3, respectively. All authors discussed the results, wrote, and commented on the manuscript.

* jrondinelli@northwestern.edu

[1] R. M. Martin, *Electronic structure: Basic theory and practical methods* (Cambridge University Press, 2004).
[2] S. Baroni, P. Giannozzi, and E. Isaev, Rev. Mineral. Geochem. **71**, 39 (2010).
[3] A. Togo, L. Chaput, I. Tanaka, and G. Hug, Phys. Rev. B **81**, 174301 (2010).
[4] A. Togo and I. Tanaka, Scr. Mater. **108**, 1 (2015).
[5] D. Alfè, G. D. Price, and M. J. Gillan, Phys. Rev. B **64**, 045123 (2001).
[6] G. J. Ackland, J. Phys.: Condens. Matter **14**, 2975 (2002).
[7] L. Vočadlo and D. Alfè, Phys. Rev. B **65**, 214105 (2002).
[8] B. Grabowski, L. Ismer, T. Hickel, and J. Neugebauer, Phys. Rev. B **79**, 134106 (2009).
[9] B. Grabowski, T. Hickel, and J. Neugebauer, Phys. Status Solidi B **248**, 1295 (2011).
[10] O. Hellman, I. A. Abrikosov, and S. I. Simak, Phys. Rev. B **84**, 180301 (2011).
[11] L. T. Kong, J. F. Li, Q. W. Shi, H. J. Huang, and Z. K., Europhys. Lett. **97**, 56004 (2012).
[12] O. Hellman, P. Steneteg, I. A. Abrikosov, and S. I. Simak, Phys. Rev. B **87**, 104111 (2013).
[13] P. Souvatzis, O. Eriksson, M. I. Katsnelson, and S. P. Rudin, Phys. Rev. Lett. **100**, 095901 (2008).
[14] P. Souvatzis, O. Eriksson, M. Katsnelson, and S. Rudin, Comput. Mater. Sci. **44**, 888 (2009).
[15] B. Rousseau and A. Bergara, Phys. Rev. B **82**, 104504 (2010).
[16] I. Errea, B. Rousseau, and A. Bergara, Phys. Rev. Lett. **106**, 165501 (2011).
[17] I. Errea, M. Calandra, and F. Mauri, Phys. Rev. Lett. **111**, 177002 (2013).
[18] K. H. Michel, S. Costamagna, and F. M. Peeters, Phys. Rev. B **91**, 134302 (2015).
[19] B. Monserrat, N. D. Drummond, and R. J. Needs, Phys. Rev. B **87**, 144302 (2013).
[20] J. Hafner, J. Comput. Chem. **29**, 2044 (2008).
[21] G. Kresse, J. Furthmüller, and J. Hafner, Europhys. Lett. **32**, 729 (1995).
[22] K. Parlinski, Z. Q. Li, and Y. Kawazoe, Phys. Rev. Lett. **78**, 4063 (1997).
[23] S. Baroni, S. de Gironcoli, A. Dal Corso, and P. Giannozzi, Rev. Mod. Phys. **73**, 515 (2001).
[24] P. Giannozzi, S. Baroni, N. Bonini, M. Calandra, R. Car, C. Cavazzoni, D. Ceresoli, G. L. Chiarotti, M. Cococcioni, I. Dabo, A. Dal Corso, S. de Gironcoli, S. Fabris, G. Fratesi, R. Gebauer, U. Gerstmann, C. Gougoussis, A. Kokalj, M. Lazzeri, L. Martin-Samos, N. Marzari, F. Mauri,

R. Mazzarello, S. Paolini, A. Pasquarello, L. Paulatto, C. Sbraccia, S. Scandolo, G. Sclauzero, A. P. Seitsonen, A. Smogunov, P. Umari, and R. M. Wentzcovitch, J. Phys.: Condens. Matter **21**, 395502 (2009).
[25] B. Beverskog and I. Puigdomenech, Corrosion Sci. **38**, 2121 (1996).
[26] B. Beverskog and I. Puigdomenech, Corrosion Sci. **39**, 107 (1997).
[27] B. Beverskog and I. Puigdomenech, Corrosion Sci. **39**, 969 (1997).
[28] B. Beverskog and I. Puigdomenech, J. Electrochem. Soc. **144**, 3476 (1997).
[29] B. Beverskog and I. Puigdomenech, Corrosion Sci. **39**, 43 (1997).
[30] J. Chivot, L. Mendoza, C. Mansour, T. Pauporté, and M. Cassir, Corrosion Sci. **50**, 62 (2008).
[31] A. Belsky, M. Hellenbrandt, V. L. Karen, and P. Luksch, Acta Crystallogr. B **58**, 364 (2002), the online database can be found on https://icsd.fiz-karlsruhe.de.
[32] A. Jain, S. P. Ong, G. Hautier, W. Chen, W. D. Richards, S. Dacek, S. Cholia, D. Gunter, D. Skinner, G. Ceder, and K. A. Persson, APL Mater. **1**, 011002 (2013), the online database can be found on https://materialsproject.org.
[33] J. Saal, S. Kirklin, M. Aykol, B. Meredig, and C. Wolverton, JOM **65**, 1501 (2013), the online database can be found on http://oqmd.org.
[34] A. R. Oganov and C. W. Glass, J. Chem. Phys. **124**, 244704 (2006).
[35] Y. Wang, J. Lv, L. Zhu, and Y. Ma, Phys. Rev. B **82**, 094116 (2010).
[36] X. Wang, T. Tsuchiya, and A. Hase, Nat. Geosci. **8**, 556 (2015).
[37] S. B. Maisel, M. Höfler, and S. Müller, Nature **491**, 740 (2012).
[38] X.-q. Li, J.-j. Zhao, and J.-c. Xu, Front. Phys. **7**, 360 (2012).
[39] X.-L. Yuan, M.-A. Xue, W. Chen, and T.-Q. An, Front. Phys. **9**, 219 (2014).
[40] J. M. Rondinelli, S. J. May, and J. W. Freeland, MRS Bulletin **37**, 261 (2012).
[41] N. A. Benedek, J. M. Rondinelli, H. Djani, P. Ghosez, and P. Lightfoot, Dalton Trans. **44**, 10543 (2015).
[42] J. Young, A. Stroppa, S. Picozzi, and J. M. Rondinelli, J. Phys.: Condens. Matter **27**, 283202 (2015).
[43] S. Curtarolo, W. Setyawan, G. L. W. Hart, M. Jahnatek, R. V. Chepulskii, R. H. Taylor, S. Wang, J. Xue, K. Yang, O. Levy, M. J. Mehl, H. T. Stokes, D. O. Demchenko, and D. Morgan, Comput. Mater. Sc. **58**, 218 (2012).
[44] S. Curtarolo, G. L. W. Hart, M. B. Nardelli, N. Mingo, S. Sanvito, and O. Levy, Nat. Mater. **12**, 191 (2013).
[45] J. M. Rondinelli, K. R. Poeppelmeier, and A. Zunger, APL Mater. **3**, 080702 (2015).
[46] J. M. Rondinelli and E. Kioupakis, Ann. Rev. Mater. Res. (2015), 10.1146/annurev-matsci-070214-021150.
[47] L. F. Huang, P. L. Gong, and Z. Zeng, Phys. Rev. B **90**, 045409 (2014).
[48] D. C. Wallace, *Thermodynamics of Crystals* (Dover Publications, Mineola, New York, 1998).
[49] J. Xie, S. de Gironcoli, S. Baroni, and M. Scheffler, Phys. Rev. B **59**, 965 (1999).
[50] N. Mounet and N. Marzari, Phys. Rev. B **71**, 205214 (2005).
[51] G. D. Barrera, J. A. O. Bruno, T. H. K. Barron, and N. L. Allan, J. Phys.: Condens. Matter **17**, R217 (2005).
[52] A. Debernardi, M. Alouani, and H. Dreyssé, Phys. Rev. B **63**, 064305 (2001).
[53] L. F. Huang and Z. Zeng, J. Appl. Phys. **113**, 083524 (2013).
[54] L. F. Huang, T. F. Cao, P. L. Gong, and Z. Zeng, Solid State Commun. **190**, 5 (2014).
[55] L. F. Huang and Z. Zeng, J. Phys. Chem. C **119**, 18779 (2015).
[56] L. F. Huang, P. L. Gong, and Z. Zeng, Phys. Rev. B **91**, 205433 (2015).
[57] S. L. Shang, Y. Wang, D. E. Kim, and Z. K. Liu, Comput. Mater. Sci. **47**, 1040 (2010).
[58] Y. Wang, J. J. Wang, H. Zhang, V. R. Manga, S. L. Shang, L. Q. Chen, and Z. Q. Liu, J. Phys.: Condens. Matter **22**, 225404 (2010).
[59] J. F. Nye, *Physical properties of crystals: their representation by tensors and matrices* (Oxford university press, Oxford, 1985).
[60] Y. Wang, Z.-K. Liu, and L.-Q. Chen, Acta Mater. **52**, 2665 (2004).
[61] B. Grabowski, T. Hickel, and J. Neugebauer, Phys. Rev. B **76**, 024309 (2007).
[62] F. Körmann, A. Dick, B. Grabowski, B. Hallstedt, T. Hickel, and J. Neugebauer, Phys. Rev. B **78**, 033102 (2008).
[63] Y. Wang, L. G. Hector Jr., H. Zhang, S. L. Shang, L. Q. Chen, and Z. K. Liu, J. Phys.: Condens. Matter **21**, 326003 (2009).
[64] Y. Wang, S. L. Shang, H. Zhang, L. Q. Chen, and Z. Q. Liu, Philos. Mag. Lett. **90**, 851 (2010).
[65] S.-L. Shang, J. E. Saal, Z.-G. Mei, Y. Wang, and Z.-K. Liu, J. Appl. Phys. **108**, 123514 (2010).
[66] S. L. Shang, Y. Wang, and Z. K. Liu, Phys. Rev. B **82**, 014425 (2010).
[67] B. Alling, T. Marten, and I. A. Abrikosov, Phys. Rev. B **82**, 184430 (2010).
[68] B. Alling, T. Marten, and I. A. Abrikosov, Nat. Mater. **9**, 283 (2010).
[69] Y. Wang, S. L. Shang, L. Q. Chen, and Z. K. Liu, Int. J. Quantum Chem. **111**, 3565 (2011).
[70] Z. K. Liu, Y. Wang, and S. L. Shang, Scr. Mater. **65**, 664 (2011).
[71] F. Körmann, A. Dick, B. Grabowski, T. Hickel, and J. Neugebauer, Phys. Rev. B **85**, 125104 (2012).
[72] P. Steneteg, B. Alling, and I. A. Abrikosov, Phys. Rev. B **85**, 144404 (2012).
[73] F. Körmann, B. Grabowski, B. Dutta, T. Hickel, L. Mauger, B. Fultz, and J. Neugebauer, Phys. Rev. Lett. **113**, 165503 (2014).
[74] A. van de Walle and G. Ceder, Rev. Mod. Phys. **74**, 11 (2002).
[75] G. Kresse and J. Furthmüller, Comput. Mater. Sci. **6**, 15 (1996).
[76] G. Kresse and J. Furthmüller, Phys. Rev. B **54**, 11169 (1996).
[77] P. E. Blöchl, Phys. Rev. B **50**, 17953 (1994).
[78] G. Kresse and D. Joubert, Phys. Rev. B **59**, 1758 (1999).
[79] J. P. Perdew, A. Ruzsinszky, G. I. Csonka, O. A. Vydrov, G. E. Scuseria, L. A. Constantin, X. Zhou, and K. Burke, Phys. Rev. Lett. **100**, 136406 (2008).
[80] J. P. Perdew, A. Ruzsinszky, G. I. Csonka, O. A. Vydrov, G. E. Scuseria, L. A. Constantin, X. Zhou, and K. Burke, Phys. Rev. Lett. **102**, 039902 (2009).

[81] L.-F. Huang and J. M. Rondinelli, Phys. Rev. B **92**, 245126 (2015).
[82] S. Shang, Y. Wang, and Z. K. Liu, Phys. Rev. B **75**, 024302 (2007).
[83] S. L. Shang, H. Zhang, Y. Wang, and Z. K. Liu, J. Phys.: Condens. Matter **22**, 375403 (2010).
[84] M. S. Senn, A. Bombardi, C. A. Murray, C. Vecchini, A. Scherillo, X. Luo, and S. W. Cheong, Phys. Rev. Lett. **114**, 035701 (2015).
[85] B. Montanari and N. M. Harrison, J. Phys.: Condens. Matter **16**, 273 (2004).
[86] E. Shojaee and M. R. Mohammadizadeh, J. Phys.: Condens. Matter **22**, 015401 (2010).
[87] P. D. Mitev, K. Hermansson, B. Montanari, and K. Refson, Phys. Rev. B **81**, 134303 (2010).
[88] B. J. Skinner, American Mineralogist **42**, 39 (1957).
[89] D. F. Gibbons, Phys. Rev. **112**, 136 (1958).
[90] A. C. Victor, J. Chem. Phys. **36**, 1903 (1962).
[91] J. B. Wachtman, T. G. Scuderi, and G. W. Cleek, J. Am. Ceram. Soc. **45**, 319 (1962).
[92] A. Schauer, Canadian J. Phys. **43**, 523 (1965).
[93] H. Ibach, Phys. Status Solidi B **31**, 625 (1969).
[94] H. J. McSkimin and P. Andreatch, J. Appl. Phys. **43**, 2944 (1972).
[95] B. Yates, R. F. Cooper, and A. F. Pojur, J. Phys. C: Solid State Phys. **5**, 1046 (1972).
[96] W. M. Yim and R. J. Paff, J. Appl. Phys. **45**, 1456 (1974).
[97] G. A. Slack and S. F. Bartram, J. Appl. Phys. **46**, 89 (1975).
[98] K. G. Lyon, G. L. Salinger, C. A. Swenson, and G. K. White, J. Appl. Phys. **48**, 865 (1977).
[99] R. B. Roberts, J. Phys. D: Appl. Phys. **14**, L163 (1981).
[100] Y. Okada and Y. Tokumaru, J. Appl. Phys. **56**, 314 (1984).
[101] D. J. Pickrell, K. A. Kline, and R. E. Taylor, Appl. Phys. Lett. **64**, 2353 (1994).
[102] R. G. Munro, J. Am. Ceram. Soc. **80**, 1919 (1997).
[103] M. W. Chase, *NIST-JANAF Thermochemical Tables (4th Ed.)* (American Institute of Physics, New York, 1998).
[104] T. Sato, K. Ohashi, T. Sudoh, K. Haruna, and H. Maeta, Phys. Rev. B **65**, 092102 (2002).
[105] H. Watanabe, N. Yamada, and M. Okaji, Int. J. Thermophysics **25**, 221 (2004).
[106] S. Kondo, K. Tateishi, and N. Ishizawa, Jpn. J. Appl. Phys. **47**, 616 (2008).
[107] S. Stoupin and Y. V. Shvyd'ko, Phys. Rev. Lett. **104**, 085901 (2010).
[108] C. Giles, C. Adriano, A. Freire Lubambo, C. Cusatis, I. Mazzaro, and M. Goncalves Hönnicke, J. Synchrotron Rad. **12**, 349 (2005).
[109] J. Thewlis and A. R. Davey, Philos. Mag. **1**, 409 (1956).
[110] R. R. Reeber and K. Wang, J. Electron. Mater. **25**, 63 (1996).
[111] I. Levin and D. Brandon, J. Am. Ceram. Soc. **81**, 1995 (1998).
[112] J. M. Andersson, *Controlling the formation and stability of alumina phases*, Ph.D. thesis, Linköpings Universitet, Linköpings, Sweden (2005).
[113] L. F. Huang, B. Grabowski, E. McEniry, D. R. Trinkle, and J. Neugebauer, Phys. Status Solidi B **252**, 1907 (2015).
[114] A. J. Falzone and F. D. Stacey, Phys. Chem. Minerals **8**, 212 (1982).
[115] P. C. Trivedi, J. Phys. C: Solid State Physics **18**, 983 (1985).
[116] H.-M. Kagaya and T. Soma, Solid State Commun. **85**, 617 (1993).
[117] H. M. Kagaya, N. Shoji, and T. Soma, Phys. Status Solidi B **142**, K13 (1987).
[118] A. Jayaraman, Rev. Mod. Phys. **55**, 65 (1983).
[119] R. Boehler, Rev. Geophys. **38**, 221 (2000).
[120] R. J. Hemley and H.-K. Mao, Int. Geol. Review **43**, 1 (2001).
[121] M. McMahon, Phil. Trans. R. Soc. A **373**, 20130158 (2015).
[122] N. A. Benedek and C. J. Fennie, Phys. Rev. Lett. **106**, 107204 (2011).
[123] Y. S. Oh, X. Luo, F.-T. Huang, Y. Wang, and S.-W. Cheong, Nat. Mater. **14**, 407 (2015).